

# Small-angle neutron scattering diffractometer at Dhruva reactor

V. K. Aswal and P. S. Goyal\*

*A small-angle neutron scattering (SANS) diffractometer has been recently installed at the guide hall of the Dhruva reactor at Trombay. The diffractometer uses a BeO filter as the monochromator. The mean wavelength of the incident neutron beam is 5.2 Å, with a wavelength resolution of approximately 15%. The angular divergence of the incident beam is  $\pm 0.5^\circ$  and the beam size at the sample position is 1.5 cm  $\times$  1.0 cm. The scattered neutrons are detected in an angular range of 1–15° using a linear He<sup>3</sup> position-sensitive gas detector. The  $Q$  range of the diffractometer is 0.018–0.32 Å<sup>-1</sup>. The diffractometer is well suited for the study of a wide variety of systems having characteristic dimensions between 10 and 150 Å. This paper gives the design features and the resolution function of SANS diffractometer.*

THERMAL neutrons (energy  $\sim 25$  meV) from nuclear reactors or accelerator-based neutron sources are now routinely used for studying the microscopic structure and dynamics of the condensed matter. Neutron scattering, in fact, consists of a family of techniques and different techniques explore the different aspects of structure and dynamics of the materials. The technique of small-angle neutron scattering (SANS) is used for studying the structure of a material on length scale of 10 to 1000 Å (refs 1, 2). In particular, SANS is used to study the shapes and sizes of the particles dispersed in homogeneous medium. The particle could be a macromolecule (biological molecule, polymer, micelle, etc.) in a solvent, a precipitate of material  $A$  in a matrix of another material  $B$ , a microvoid in a metal or a magnetic inhomogeneity in a nonmagnetic matrix. In suitable cases, SANS also provides information about interparticle interactions.

SANS is a diffraction experiment. It involves scattering of a monochromatic beam of neutrons from the sample and measuring the scattered neutron intensity as a function of the scattering angle. It is different from conventional diffraction experiments, where the structure of the material is examined at atomic resolution ( $\sim 1$  Å). The wave vector transfer  $Q$  ( $= 4\pi \sin \theta/\lambda$ , where  $2\theta$  is the scattering angle and  $\lambda$  is the neutron wavelength) in SANS experiments is small, typically in the range 0.001 to 1.0 Å<sup>-1</sup>. To obtain low  $Q$  values, SANS instrument uses large wavelength ( $\sim 5$  Å) neutrons and small scattering angles ( $\sim 0.5$ – $10^\circ$ ).

An indigenously developed SANS diffractometer has been operating at CIRUS reactor, Trombay for the last ten years or so<sup>3,4</sup>. This diffractometer has been used by scientists at the Bhabha Atomic Research Centre, Mumbai and university researchers<sup>5–17</sup>. With the availability of guides at the Dhruva reactor, the above SANS diffractometer has been suitably modified and installed in the guide laboratory of the reactor. The neutron flux at the Dhruva reactor ( $\sim 1.8 \times 10^{14}$  n/cm<sup>2</sup>/s) is more than that at the CIRUS reactor ( $\sim 6 \times 10^{13}$  n/cm<sup>2</sup>/s). Moreover, the guide laboratory provides an environment where the general neutron background is quite low. In view of these two facts and the modifications in the instrument, the SANS diffractometer at Dhruva provides data which are of much better quality than those obtained earlier at CIRUS. This paper gives the details of the SANS diffractometer, which is now operating at the Dhruva reactor. The effect of instrumental resolution function as obtained using Monte Carlo simulations has also been discussed. The plan of the paper is as follows. First, we give a general discussion on the design of a SANS diffractometer in the next section. The design features of the SANS diffractometer at Dhruva are then given, followed by details of the instrumental resolution function. Next, the calibration procedures and the results of the typical measurements are discussed. In the end, a summary is given.

## Design of a SANS diffractometer

As already mentioned, SANS experiment involves scattering of a monochromatic beam of neutrons from a sample and measuring the scattered neutron intensity as a function of scattering angle. Figure 1 gives a schematic representation of the essential features of a SANS instrument<sup>18</sup>.

V. K. Aswal is in the Solid State Physics Division, Bhabha Atomic Research Centre, Mumbai 400 085, India; P. S. Goyal is in the Inter-University Consortium for Department of Atomic Energy Facilities, Mumbai Centre, Bhabha Atomic Research Centre, Mumbai 400 085, India.

\*For correspondence. (e-mail: psgoyal@magnum.barc.ernet.in)

Neutrons emerge from the beam tube of a reactor with nearly Maxwellian spectrum whose characteristic temperature depends on the moderator temperature  $T_m$ . A slice of this distribution is transmitted by the monochromator system—and enters the flight path  $L_1$  with angular limits defined by the radii  $R_{ns}$  and  $R_s$ , of the source and sample apertures, respectively. The direct and scattered beams pass through a second flight tube  $L_2$  and impinge on the detector plane. A carefully positioned beam stop masks the detector from the direct beam. Usually SANS instruments use one-dimensional or two-dimensional position sensitive detectors.  $\Delta l$  is the pixel size of the detector. The scattering angle corresponding to the  $n$ th pixel is  $2\theta = \tan^{-1}(n\Delta l/L_2)$ . The main considerations in designing the SANS diffractometer are<sup>18</sup>:

- (i) To get reasonable intensities, the sample size and the detector pixel size are kept large ( $\sim 1$  cm). Further, it is recommended that the sizes of the sample slit and the detector pixel should be comparable ( $R_s \sim \Delta l$ ).
- (ii) As the scattering angles involved are small ( $2\theta \sim 1^\circ$ ), it is important that beam divergences are kept as small as possible. This is achieved by using large values ( $\sim 5$  m) for flight paths  $L_1$  and  $L_2$ . The optimization of intensity and resolution suggests that one should have  $R_s = \Delta l$ ,  $R_{ns} = 2R_s$  and  $L_1 = L_2$ .
- (iii) To obtain low  $Q$  values at manageable scattering angles, SANS instruments use large wavelength ( $\lambda \geq 4$  Å) neutrons.
- (iv) The  $Q$  resolution of a SANS diffractometer depends on uncertainties in the scattering angle and the incident wavelength. It is given by

$$\frac{\Delta Q}{Q} = \left[ \left( \frac{\Delta\theta}{\theta} \right)^2 + \left( \frac{\Delta\lambda}{\lambda} \right)^2 \right]^{1/2}. \quad (1)$$

The uncertainty  $\Delta\theta$  in angle depends on the sizes of the

slits and the detector pixel and the distances  $L_1$  and  $L_2$ . SANS instruments have typically  $\Delta\theta/\theta \sim 0.1$ . Thus these instruments require only moderately monochromated beams ( $\Delta\lambda/\lambda \sim 0.1$ ). The single crystal monochromators used in conventional diffractometers provide  $\Delta\lambda/\lambda \sim 0.02$  and are thus not suitable for SANS instruments. SANS instruments use (a) velocity selector<sup>19</sup>, (b) polycrystalline BeO filter<sup>4</sup>, (c) double crystal monochromator<sup>20</sup> or (d) several misaligned crystals<sup>21</sup> in a dog-leg configuration for a monochromator. The relative merits of these monochromators have been discussed in our earlier paper<sup>22</sup>.

### SANS diffractometer at Dhruva

The schematic of the SANS diffractometer at the Dhruva reactor is shown in Figure 2. The diffractometer has been installed on guide G1 in the guide laboratory of the Dhruva reactor at Trombay. This guide has cut-off wavelength  $\lambda^* = 2.2$  Å and presently it looks at the thermal moderator of the reactor<sup>23</sup>. The details of the various components of the diffractometer are given now.

#### Monochromator

The monochromator consists of a polycrystalline BeO filter, which has a Bragg cut-off at 4.7 Å. The neutron beam from the guide is allowed to pass through a 15 cm long block of the BeO filter. Neutrons having wavelengths larger than 4.7 Å pass through the BeO filter and those having wavelengths smaller than 4.7 Å are Bragg scattered. In this way one obtains a nearly-monochromatic beam. The wavelength distribution [ $I(\lambda)$  vs  $\lambda$ ] of the filtered beam as measured using a mica crystal mounted at the sample position is shown in Figure 3. The mean wavelength of the distribution is 5.2 Å and has a spread ( $\Delta\lambda/\lambda$ )

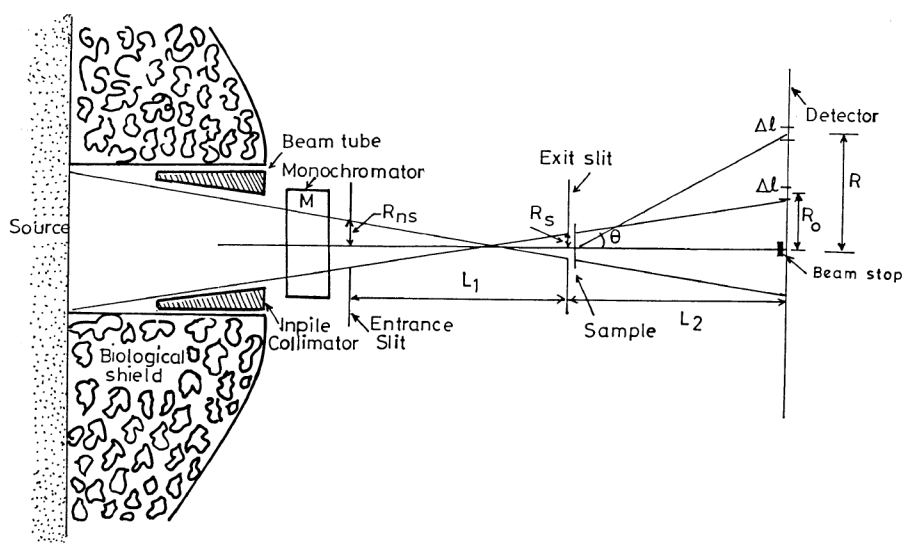


Figure 1. Schematic representation of a SANS instrument.

of about 15%. The BeO filter is kept at liquid-nitrogen temperature. Because of a decrease in thermal diffuse scattering, the intensity of the transmitted beam increases by a factor of 1.5 when the filter is cooled from room temperature to the liquid-nitrogen temperature.

It may be mentioned that in the near future, a double crystal monochromator will be installed to improve the wavelength resolution of the instrument. The double crystal monochromator has been fabricated and tested for this purpose<sup>22</sup>. This monochromator has a better wavelength resolution of about 5% at  $\lambda = 4.75 \text{ \AA}$  and the wavelength distribution is symmetric about the mean wavelength. The use of this monochromator will, however, reduce the neutron intensity by a factor of about 4.

### Collimation

The collimator system between the monochromator and the sample consists of two rectangular slits  $S_1$  ( $3.0 \text{ cm} \times 2.0 \text{ cm}$ ) and  $S_2$  ( $1.5 \text{ cm} \times 1.0 \text{ cm}$ ) separated by a distance of 2 m. The beam size at the sample position is  $1.5 \text{ cm} \times 1.0 \text{ cm}$ . This collimator gives an angular divergence of  $\pm 0.5^\circ$  of the incident beam. The measured incident neutron flux at the sample position is  $2.2 \times 10^5 \text{ n/cm}^2/\text{s}$ .

### Sample table

A squarish  $10 \text{ cm} \times 10 \text{ cm}$  sample table has been provided to mount the sample. It can take a load of a small cryostat or a heater. The height of the sample can be adjusted depending on the requirement. Solid pellet-like samples or quartz sample holders of different thicknesses for liquid samples can be mounted on the sample table. A low efficiency monitor detector resides at the outer edge of incident beam just before the slit  $S_2$ . SANS distribu-

tions are usually recorded for a fixed monitor count. As the reactor power could fluctuate during an experiment, it is not adequate to record the SANS measurements from different samples for identical times for the purpose of normalizing these data. However, when measurements for different samples are made for identical monitor counts, one ensures that different sets of measurements correspond to the same number of incident neutrons.

### Position sensitive detector

The scattered neutrons from the sample are detected using a 100 cm long, 3.8 cm dia  $\text{He}^3$  linear position sensitive detector. The detector is housed in a massive shielding to reduce the background. The distance between the sample and the detector is 1.85 m. The detector is made up of a stainless steel tube filled with  $\text{He}^3$  gas at 30 PSI and Kr at 15 PSI pressure. Kr is added to reduce the charged particle range and hence to improve the position resolution. The coordinates of the position where neutron detection takes place are obtained using charge division method<sup>24</sup>. The position resolution of the detector is 12 mm. The detector and the beam stop are so positioned that they allow an angular range of 1 to  $15^\circ$  and a  $Q$  range of 0.018 to  $0.32 \text{ \AA}^{-1}$ .

### Resolution function of the instrument

The SANS instrument is used to measure the coherent differential scattering cross-section per unit volume  $(d\sigma/d\Omega)(Q)$  for the sample. In the actual experiment, in addition to coherent scattering, there is a small  $Q$ -independent background arising from the incoherent scattering by the sample. This background can be subtracted and is not relevant for the present discussion. The measured SANS distribution is a convolution of the theoretical  $(d\sigma/d\Omega)(Q)$  and the resolution function of the instrument. Thus one has to take account of these resolution effects

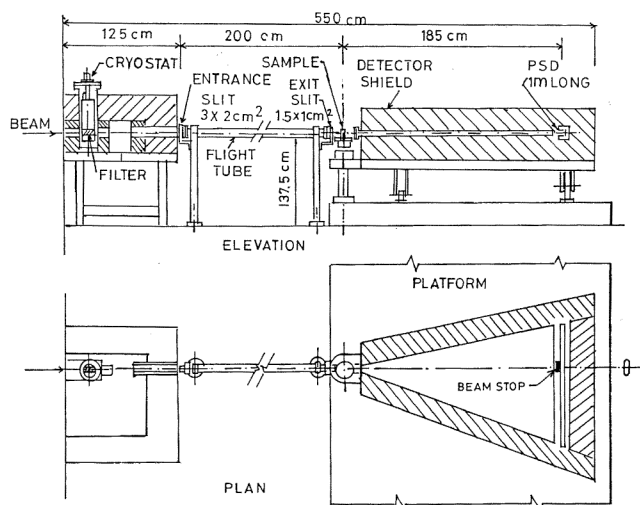


Figure 2. Schematic of the SANS diffractometer at Dhruva reactor.

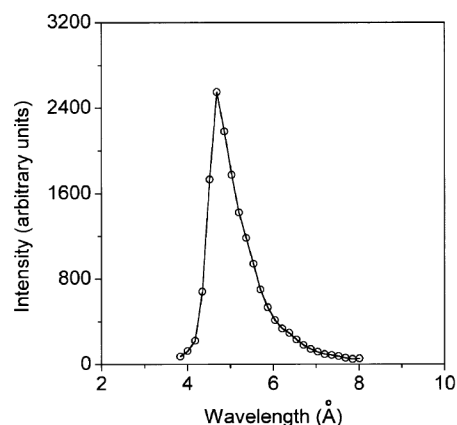


Figure 3. Measured wavelength distribution of the BeO filtered neutron beam.

while comparing the calculated and the measured distributions.

There are three components to the resolution function for the diffractometer. These contributions arise from the finite collimation, the wavelength distribution and the spatial resolution of the detector. When the diffractometer is set to detect neutrons with wave vector transfer  $Q$ , neutrons with wave vector transfers  $Q'$  in the neighbourhood of  $Q$  also contribute to the scattering due to the finite instrument resolution. If we describe the resolution function of the diffractometer by  $R(Q, Q')$  at the wave vector transfer  $Q$ , the measured intensity  $I(Q)$  is related to the scattering cross-section  $(d\sigma/d\Omega)(Q)$  by the integral<sup>25</sup>:

$$I(Q) = \int R(Q, Q') \frac{d\sigma}{d\Omega}(Q') dQ'. \quad (2)$$

We have determined the resolution function by the Monte Carlo simulations. For this, we assume the neutron source to be a uniform neutron beam emerging from the guide. The neutrons are generated randomly in space from this source. We assign these neutrons the wavelength distribution as given by the measured wavelength distribution. After that, only those neutrons passing through the slits and reaching at the sample are considered. To get the resolution function at different  $Q$  values, the neutrons are scattered from the sample following a scattering law of the type  $\delta(Q' - Q)$ . The scattered neutrons reach the detector but their position is uncertain to the extent of the detector resolution. The detector resolution has a Gaussian distribution (FWHM = 12 mm) and the neutrons are recorded with this distribution at the detector.

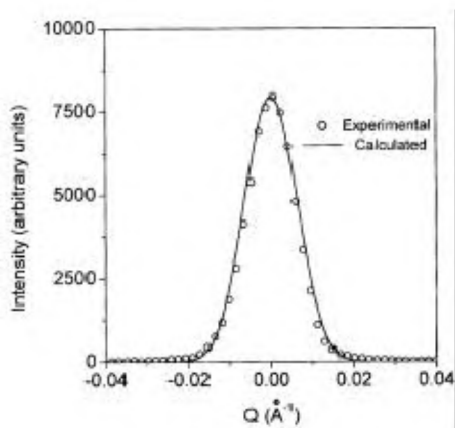
Figure 4 shows the comparison of the measured and the calculated direct beam profiles at the detector. The direct beam was measured by the detector after removing the beam stop. It is seen that the measured and the calculated profiles agree well with each other.

Figure 5 shows resolution function at  $Q = 0.05 \text{ \AA}^{-1}$ . The resolution  $\Delta Q/Q$  is about 40%. Similar calculations were

done for several  $Q$  values. The variation of FWHM of the resolution function with  $Q$  is shown in Figure 6. The solid curve in the figure is the fitted quadratic function to the results of the Monte Carlo simulations at different  $Q$  values. It is found that FWHM of the resolution function varies as  $\Delta Q = 0.0151 + 0.0692Q + 0.1603Q^2$ . The contributions to the resolution function from wavelength distribution ( $\Delta Q_\lambda$ ), collimation ( $\Delta Q_\theta$ ) and the spatial resolution of the detector ( $\Delta Q_D$ ) are also shown in Figure 6.  $\Delta Q_\lambda$  depends linearly on  $Q$ . It is negligible at small  $Q$  values but dominates at large  $Q$  values. It is because of this and the asymmetric wavelength distribution of the monochromated beam that the calculated resolution function becomes more asymmetric with increase in  $Q$ . It may be mentioned that the use of double crystal monochromator system, where wavelength distribution is symmetric in  $\lambda$ , would provide a resolution function which is symmetric over the entire  $Q$  range. The contribution of  $\Delta Q_\theta$  to the resolution function is independent of  $Q$  and has the major contribution at small  $Q$  values.  $\Delta Q_D$  is also independent of  $Q$ .

### Instrument calibration and performance

Data from the position sensitive detector are stored in a multichannel analyser as intensity vs channel number. There is a one to one correspondence between the channel number and the distance  $R$  between the point of neutron detection and the centre of the incident beam at the detector. The scattering angle is given by  $2\theta = \tan^{-1}(R/L_2)$ , where  $L_2$  is the distance between the sample and the detector. Thus each channel of the multichannel analyser is related to the corresponding  $Q$  value. In a SANS experiment, in addition to recording the intensity distribution  $I_s(Q)$  with the sample, one has to measure two types of backgrounds  $I_b(Q)$  and  $I_c(Q)$ . The room background  $I_b(Q)$  is measured by putting cadmium at the sample position.  $I_c(Q)$  is the residual part of the direct beam and is meas-



**Figure 4.** Comparison of measured direct beam profile with calculated profile from Monte Carlo simulations.

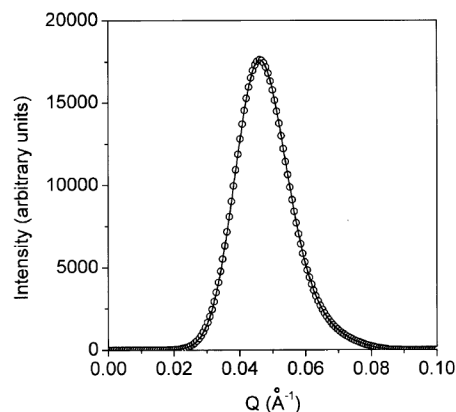


**Figure 5.** Calculated resolution function of the SANS diffractometer at  $Q = 0.05 \text{ \AA}^{-1}$ .

ured without any sample in the beam or by having an empty sample holder at the sample position in case such a holder is used in the experiment. The measured intensity from the sample  $I_s(Q)$  is corrected for these contributions. The corrected scattered intensity  $I(Q)$  of interest from the sample is given by<sup>26</sup>

$$I(Q) = \left[ \frac{I_s(Q) - I_b(Q)}{T_s} - \frac{I_e(Q) - I_b(Q)}{T_e} \right] T_s. \quad (3)$$

Here  $T_s$  is the sample transmission and  $T_e$  is the transmission of the empty sample holder.  $I_s(Q)$ ,  $I_b(Q)$  and  $I_e(Q)$  in eq. (3) correspond to identical monitor counts. Figure 7 shows typical measured raw distribution  $I_s(Q)$  for 0.1 M cetyltrimethylammonium bromide (CTAB) micellar solution in  $D_2O$  as obtained using SANS diffractometer at the Dhruva reactor. The empty sample holder and beam-blocked background are also shown. We had carried out SANS experiments on the CTAB sample earlier using the CIRUS instrument<sup>4,8</sup>. Figure 7 shows that the SANS distribution from CTAB micellar solution obtained at Dhruva is in good agreement with the data taken at the CIRUS instrument. However, the counting time at the CIRUS instrument was about 15 times greater compared to that at Dhruva. This shows that the SANS diffractometer at Dhruva is 15 times more efficient compared to that at the CIRUS instrument. Further, it was seen that the beam-blocked background at the Dhruva instrument is half of that at the CIRUS instrument and thus the signal to noise ratio has improved by a factor of 30.

It may be noted that though the flux at the Dhruva reactor is only 3 times that of the CIRUS reactor, we obtain a gain of about 15 in throughput at Dhruva compared to that at CIRUS reactor. We have not been able to quantitatively

understand the reasons for higher intensity at the Dhruva instrument. However, this could arise because of several reasons. Firstly, one had to use Bi plug in the CIRUS instrument to cut down the  $\gamma$ -ray background. At Dhruva, the use of curved guide ensures that the sample does not see the direct beam, and thus there is no need to use a Bi plug. The BeO filter at CIRUS was inside the beam hole and it was not convenient to cool it. However, now BeO is outside and is cooled to liquid-nitrogen temperature. Moreover, as the fast neutron flux in the beam from the guide is quite small, one is able to reduce the length of the BeO filter from 25 to 15 cm, which results in higher transmission of the neutrons. The above factors and perhaps better alignment, etc. have resulted in a 15 times higher intensity at the Dhruva instrument compared to that at the CIRUS instrument.

In a SANS experiment, the sample is usually taken in the form of a plate (circular or rectangular), so that it has uniform thickness over the beam area. If  $(d\sigma/d\Omega)(Q)$  is the differential scattering cross-section per unit volume of the sample, the measured scattered neutron intensity is given by<sup>27</sup>:

$$I(Q) = K T_s t \frac{d\sigma}{d\Omega}(Q), \quad (4)$$

where  $t$  is the sample thickness and  $K$  a constant which depends on instrumental parameters such as incident neutron flux, detector efficiency, solid angle subtended by detector element at sample position, etc.

By combining eqs (3) and (4), we get the following expression for the scattering cross-section of the sample:

$$\frac{d\sigma}{d\Omega}(Q) = \frac{1}{Kt} \left[ \frac{I_s(Q) - I_b(Q)}{T_s} - \frac{I_e(Q) - I_b(Q)}{T_e} \right]. \quad (5)$$

The instrumental constant  $K$  is determined by recording

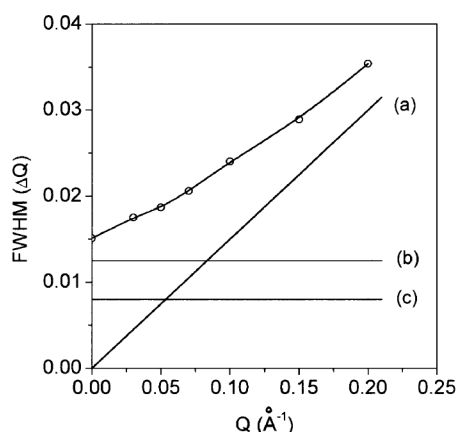


**Figure 6.** Variation of the FWHM of the resolution function with  $Q$ . The open circles are results from the Monte Carlo simulations and the solid curve is the fitted quadratic function. Three contributions to the instrumental resolution arising from (a) wavelength distribution ( $\Delta Q_\lambda$ ), (b) collimation ( $\Delta Q_\theta$ ) and (c) spatial resolution of the detector ( $\Delta Q_D$ ) are also shown.

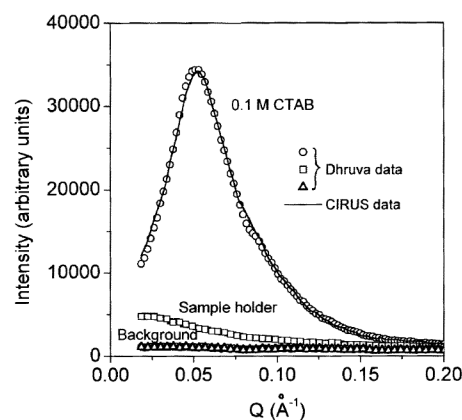


**Figure 7.** Typical SANS distributions measured using SANS diffractometer at Dhruva reactor. Data from 0.1 M CTAB micellar solution taken at CIRUS reactor are also shown for comparison after normalizing with Dhruva data.

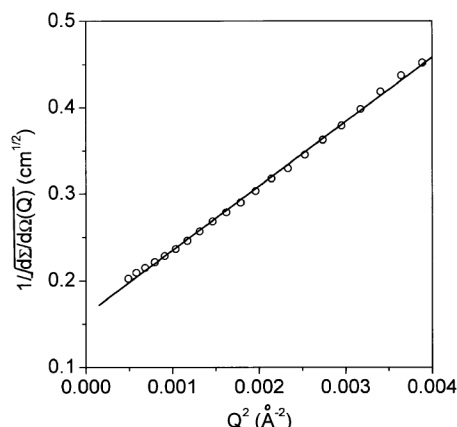


Figure 8. Debye-Bueche plot of the porous silica sample (Porasil-A11).

the data from a standard sample (e.g. H<sub>2</sub>O, vanadium, Porasil-A11, etc.)<sup>27</sup>. The measurement thus provides  $(d\sigma/d\Omega)(Q)$  in absolute units, namely cm<sup>-1</sup>.

We have calibrated the present SANS diffractometer using a porous silica sample for which, to a good approximation, the scattering is given by the Debye-Bueche formula<sup>27</sup>:

$$\frac{d\Sigma}{d\Omega}(Q) = \frac{d\Sigma}{d\Omega}(0) \frac{1}{(1 + Q^2 a^2)^2}, \quad (6)$$

where  $a$  is the correlation length and is the measure of the extension of the porosity<sup>28</sup>. SANS distributions from the Porasil-A11 sample using the above diffractometer and the SANS diffractometer at Oak Ridge National Laboratory, USA were obtained. Comparison of the two data gave the value of the instrumental constant  $K$ . Figure 8 shows a Debye-Bueche plot of the scattering from Porasil-A11 sample measured using SANS diffractometer at the Dhruva reactor. The fit using eq. (6) gives  $(d\sigma/d\Omega)(0) = 39.0 \text{ cm}^{-1}$  and correlation length  $a = 20.6 \text{ \AA}$ . The data taken at Oak Ridge National Laboratory gave  $(d\sigma/d\Omega)(0) = 43.8 \text{ cm}^{-1}$  and  $a = 21.8 \text{ \AA}$ . We find that the parameters  $(d\sigma/d\Omega)(0)$  and  $a$  are slightly lower at the Dhruva instrument and the differences are related to resolution effects. It is seen that if we take account of resolution effects, the two sets of data give similar values of  $(d\sigma/d\Omega)(0)$  and  $a$ .

Figure 9 shows the corrected SANS data from 0.1 M CTAB micellar solution using eq. (5) and their comparison with the data taken from the same system using SANS diffractometer at Intensed Pulsed Source, Argonne National Laboratory (ANL), USA<sup>29</sup>. We find that the two distributions agree well with each other. It may be mentioned that the raw ANL data were convoluted with resolution function of our diffractometer before comparing with the present data in Figure 9. SANS diffractometer at ANL has a very good  $Q$  resolution and its effect

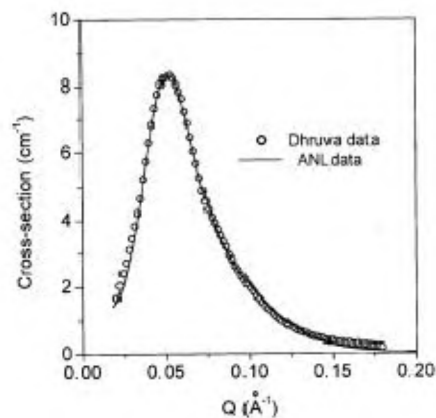


Figure 9. SANS distribution from 0.1 M CTAB micellar solution. ANL data is shown after convoluting with the resolution function of the Dhruva instrument.

to the data smearing is negligible. The above results thus show that calibration and performance of the SANS diffractometer at the Dhruva reactor are satisfactory.

## Summary

SANS is a well-established technique for examining the structure of materials on a length scale of 10 to 1000 Å. We have installed a small-angle neutron scattering diffractometer at the guide hall of the Dhruva reactor at Trombay. The diffractometer has been calibrated by recording data on standard samples. The resolution function of the diffractometer has been calculated using Monte Carlo simulations. It is seen that resolution-corrected data on CTAB micellar solutions as obtained on the above diffractometer agree very well with those taken on a SANS diffractometer at ANL, USA. The accessible  $Q$  range of the diffractometer is 0.018 to 0.32 Å<sup>-1</sup> and thus it is ideally suited for studying particle sizes in the range of 10 to 150 Å.

1. Kostorz, G., in *Treatise on Material Science and Technology* (ed. Kostorz, G.), Academic Press, New York, 1979, vol. 15.
2. Windsor, C. G., *J. Appl. Crystallogr.*, 1988, **21**, 582-588.
3. Desa, J. A. E., Mazumder, S., Sequiera A. and Dasannacharya, B. A., *Solid State Phys. C (India)*, 1985, **28**, 318.
4. Goyal, P. S., Aswal, V. K. and Joshi, J. V., BARC Report, BARC/1995/I/018.
5. Goyal, P. S., Chakravarthy, R., Dasannacharya, B. A., Desa, J. A. E., Kelkar, V. K., Manohar, C., Narasimhan, S. L., Rao, K. R. and Valaulikar, B. S., *Phys. B*, 1989, **156**, 471-473.
6. Rao, K. S., Goyal, P. S., Dasannacharya, B. A., Kelkar, V. K., Manohar, C. and Menon, S. V. G., *Pramana - J. Phys.*, 1991, **37**, 311-319.
7. Kelkar, V. K., Mishra, B. K., Rao, K. S., Goyal, P. S. and Manohar, C., *Phys. Rev. A*, 1991, **44**, 8421-8424.
8. Goyal, P. S., Menon, S. V. G., Dasannacharya, B. A. and Rajagopalan, V., *Chem. Phys. Lett.*, 1993, **211**, 559-563.
9. Prasad, C. D., Singh, H. N., Goyal, P. S. and Rao, K. S., *J. Colloid Interface Sci.*, 1993, **155**, 415-419.
10. Goyal, P. S., *Phase Transitions*, 1994, **50**, 143-176.

11. Kumar, S., Aswal, V. K., Singh, H. N., Goyal, P. S. and Kabir-ud-Din, *Langmuir*, 1994, **10**, 4069–4072.
12. Aswal, V. K., Goyal, P. S., Menon, S. V. G. and Dasannacharya, B. A., *Phys. B*, 1995, **213**, 607–609.
13. De, S., Aswal, V. K., Goyal, P. S. and Bhattacharya, S., *J. Phys. Chem.*, 1996, **100**, 11664–11671.
14. Upadhyay, T., Upadhyay, R. V., Mehta, R. V., Aswal, V. K. and Goyal, P. S., *Phys. Rev. B*, 1997, **55**, 5585–5588.
15. Aswal, V. K. and Goyal, P. S., *Phys. B*, 1998, **245**, 73–80.
16. Jain, N., Aswal, V. K., Goyal, P. S. and Bahadur, P., *J. Phys. Chem. B*, 1998, **102**, 8452–8458.
17. Aswal, V. K. and Goyal, P. S., *Phys. Rev. E*, 2000, **61**, 2947–2953.
18. Schmatz, W., Springer, T., Scelten, J. and Ibel, K., *J. Appl. Crystallogr.*, 1974, **7**, 96–116.
19. Crawford, K. and Carpenter, J. M., *J. Appl. Crystallogr.*, 1988, **21**, 589–601.
20. Child, H. R. and Spooner, S., *J. Appl. Crystallogr.*, 1980, **13**, 259–264.
21. Mildner, D. F. R., Berliner, R., Pringle, O. A. and King, J. S., *J. Appl. Crystallogr.*, 1981, **14**, 370–382.
22. Aswal, V. K., Joshi, J. V., Goyal, P. S. and Pimple, A. V., *J. Appl. Crystallogr.*, 2000, **33**, 118–125.
23. Basu, S. and Rao, L. M., *Physica B*, 1991, **174**, 409–414.
24. Convert, P. and Forsyth, J. B. (eds), *Position Sensitive Detection of Thermal Neutrons*, Academic Press, London, 1983.
25. Pedersen, J. S., Posselt, D. and Mortensen, K., *J. Appl. Crystallogr.*, 1990, **23**, 321–333.
26. Chen, S. H. and Lin, T. L., in *Methods of Experimental Physics* (eds Price, D. L. and Skold, K.), Academic Press, New York, 1987, vol. 23B, pp. 489–542.
27. Wignall, G. W. and Bates, F. S., *J. Appl. Crystallogr.*, 1987, **20**, 28–40.
28. Debye, P. and Bueche, A., *J. Appl. Phys.*, 1949, **20**, 518–525.
29. Aswal, V. K., Goyal, P. S. and Thiagarajan, P., *J. Phys. Chem. B*, 1998, **102**, 2469–2473.

ACKNOWLEDGEMENTS. We thank Dr S. K. Sikka and Dr M. Ramanadham for their interest in this work. We also thank Dr B. A. Dasannacharya and Dr A. S. Sequeira for useful discussions. The help from Mr J. V. Joshi and Mr V. M. Shah during the installation of the SANS diffractometer is acknowledged. We are grateful to Dr G. D. Wignall for providing the standard sample for the calibration of the instrument and Dr P. Thiagarajan for recording the SANS data on CTAB micellar solution at Argonne National Laboratory. Lastly, we thank the referee for useful suggestions.

Received 4 May 2000; revised accepted 30 June 2000